

Quantifying the Safety of Trajectories using Peak-Minimizing Control

Jared Miller¹, Mario Sznaiier¹

October 2, 2024

Abstract

This work quantifies the safety of trajectories of a dynamical system by the perturbation intensity required to render a system unsafe (crash into the unsafe set). In the data-driven setting, this perturbation intensity can be interpreted as the minimal data corruption required for a data-consistent model to crash. Computation of this measure of safety is posed as a peak-minimizing optimal control problem. Convergent lower bounds on the minimal peak value of controller effort are computed using polynomial optimization and the moment-Sum-of-Squares hierarchy.

1 Introduction

A trajectory starting at an initial point $x_0 \in X$ following dynamics $\dot{x} = f_0(t, x)$ is safe with respect to the unsafe set X_u in the time horizon $t \in [0, T] \subset [0, \infty)$ if there does not exist a time t' such that $x(t' | x_0)$ is a member of X_u . The set X_0 is safe with respect to X_u if all initial points $x_0 \in X_0$ generate safe trajectories. This paper quantifies the safety of trajectories by maximum control effort (Optimal Control Problem (OCP) cost) needed to crash the agent into the unsafe set. An example of this type of safety result is if tilting a car's steering wheel by a maximum extent of 3° over the course of its motion would cause the car to crash. In the data-driven framework, a trajectory is labeled safe if it would require the true system to have a large constraint violation against any of its state-derivative data observations in order to crash. The process of analyzing safety by computing the peak-minimizing-OCP cost will be referred to as 'crash safety'.

Let $W \subset \mathbb{R}^L$ be a compact input set, and let \mathcal{W} be the class of functions whose graphs satisfy $\forall t \in [0, T] : w(t) \in W$. Given a control-cost $J(w)$ (which can represent the intensity of the data corruption), we can pose the following peak-minimizing free-terminal-time OCP:

$$\begin{aligned} Q^* &= \inf_{t, x_0, w} \sup_{t' \in [0, t]} J(w(t')) \\ \dot{x}(t') &= f(t', x(t'), w(t')) & \forall t' \in [0, T] \\ x(t | x_0, w(\cdot)) &\in X_u \\ w(\cdot) &\in \mathcal{W}, t \in [0, T], x_0 \in X_0. \end{aligned} \tag{1}$$

The variables of (1) are the stopping time t , the initial condition x_0 , and the input process $w(\cdot)$. Assuming for the purposes of this introduction that $J(0) = 0$, $\forall w \neq 0 : J(w) > 0$ and that J possesses connected sublevel sets (such as J quadratic), the set x_0 is unsafe if $Q^* = 0$ because the process $w(t) = 0$ is sufficient for the trajectory to reach a terminal set of X_u . The value of a nonzero Q^* then measures the amount of control effort (perturbation intensity) needed to render the trajectory unsafe. Connected level sets are imposed to

¹J. Miller, and M. Sznaiier are with the Robust Systems Lab, ECE Department, Northeastern University, Boston, MA 02115. (e-mails: miller.jare@northeastern.edu, msznaiier@coe.neu.edu).

J. Miller and M. Sznaiier were partially supported by NSF grants ECCS-1808381 and CNS-2038493, AFOSR grant FA9550-19-1-0005, and ONR grant N00014-21-1-2431. J. Miller was in part supported by the Chateaubriand Fellowship (performed at LAAS-CNRS) of the Office for Science & Technology of the Embassy of France in the United States, and by the International Student Exchange Program from AFOSR.

add interpretability to Q^* ; a disconnected choice of J with multiple local minima could yield a large input w with a low Q^* .

A running cost $\int_0^T J(w(t'))dt$ yielding a standard-form (Lagrange) OCP may also be applied, but we elect to use a peak-minimizing cost $\max_{t'} J(w(t'))$ in order to penalize perturbation intensity. The running-cost would penalize a low-magnitude control being applied for an extended period of time, while peak-minimizing control reduces the intensity.

Peak-minimizing control problems, such as in (1), are a particular form of robust optimal control in which the minimizing agents are $(t, x_0, w(\cdot))$ and the maximizing agent is $t' \in [0, t]$. Necessary conditions for these robust programs may be found in [1]. Instances of peak-minimizing control include minimizing the maximum number of infected persons in an epidemic under budget constraints [2] and choosing flight parameters to minimize the maximum skin temperature during atmospheric reentry [3, 4]. The work in [5] outlines conversions between peak-minimizing OCPs and equivalent Mayer-form OCPs (terminal cost only).

This paper continues a sequence of research about quantifying the safety of trajectories. Unsafety can be proven using path-planning by finding a feasible pair $(t', x_0) \in [0, T] \times X_0$ such that $x(t' | x_0) \in X_u$. Barrier [6, 7] and Density functions [8] are binary certificates confirming that there does not exist an unsafe trajectory based on the satisfaction of nonnegativity constraints. Safety margins use maximin peak estimation to estimate the X_u -representing-inequality-constraint violation [9]. The distance of closest approach between a trajectory starting in X_0 and points in X_u is a more interpretable measure of safety than abstract safety margins [10]. Even so, distance estimation does not tell the full story; a trajectory may lie close to X_u in the sense of distance, but it could require a large value of Q^* to render the same trajectory unsafe.

Direct solution of OCPs using the Hamilton-Jacobi-Bellman (HJB) equation or the Pontryagin Maximum Principle may be challenging, especially when solutions do not exist in closed form [11]. These generically non-convex OCPs may be lifted into convex infinite-dimensional Linear Programs (LPs) in occupation measures [12], whose dual LP involve subvalue functions satisfying HJB inequalities. These infinite-dimensional LPs produce lower-bounds on the true OCP, with equality holding under compactness and regularity conditions. The moment-Sum of Squares (SOS) hierarchy of Semidefinite Programs (SDPs) may be used to produce a rising sequence of lower bounds to the true OCP if the dynamics $f(t, x, w)$ are polynomial and the sets (W, X, X_0, X_u) are Basic Semialgebraic (BSA) [13]. This infinite-dimensional LP and finite-dimensional SDP pattern has also been applied to reachable set estimation [14, 15], peak estimation [16, 17], and maximum controlled invariant set estimation [18].

This paper transforms program (1) into the Mayer OCP using [5], relaxes the nonconvex OCP into an infinite-dimensional LP with the same objective value [12], and then lower-bounds Q^* by using the moment-SOS hierarchy [13, 19]. The robust counterpart method of [20, 21] will be used to simplify the infinite-dimensional LP when W and the graph of J are both polytopic. Contributions of this work include,

- An interpretation of peak-minimal control costs as a quantification of safety
- An infinite-dimensional LP that produces the peak-minimal cost under compactness, regularity, and convexity conditions
- A subvalue functional that lower-bounds the crash-safety effort
- An application of crash-safety towards data-driven safety analysis

This paper has the following structure: Section 2 reviews the notations, the peak-minimizing control framework of [5], and SOS methods. Section 3 formulates an infinite-dimensional LP to solve (1). Section 4 applies the crash-safety framework towards L_∞ -penalized data-driven analysis using robust Lie counterparts from [21]. Section 5 forms SOS programs for crash-safety and tabulates their computational complexity. Section 6 evaluates the safety of points inside X by a subvalue function of the crash-safety cost. Section 7 provides demonstrations of crash-safety. Section 8 concludes the paper.

2 Preliminaries

2.1 Acronyms/Initialisms

BSA Basic Semialgebraic

HJB	Hamilton-Jacobi-Bellman
LP	Linear Program
OCP	Optimal Control Problem
PSD	Positive Semidefinite
SDP	Semidefinite Program
SOS	Sum of Squares
WSOS	Weighted Sum of Squares

2.2 Notation

The set of real numbers is \mathbb{R} and the n -dimensional real vector spaces is \mathbb{R}^n . The all-ones vector is $\mathbf{1}$. The set of natural numbers is \mathbb{N} and the set of n -dimensional multi-indices is \mathbb{N}^n . The set of natural numbers between a and b is $a..b \subset \mathbb{N}$. The cone of $n \times n$ symmetric Positive Semidefinite (PSD) matrices is \mathbb{S}_+^n .

The set of polynomials of an indeterminate x with real-valued coefficients is $\mathbb{R}[x]$. The degree of a polynomial $p \in \mathbb{R}[x]$ is $\deg p$. The vector space of polynomials up to degree $d \in \mathbb{N}$ is $\mathbb{R}[x]_{\leq d}$. The coefficients of a polynomial $p \in \mathbb{R}[x]$ are $\text{coeff}_x(p(x))$.

The ring of continuous functions over a space $S \subseteq \mathbb{R}^n$ is $C(S)$. The set of first-differentiable functions over S is $C^1(S) \subset C(S)$. The subcone of nonnegative functions over S is $C_+(S) \subset C(S)$.

The set of nonnegative Borel measures over S is $\mathcal{M}_+(S)$. Given a measure $\mu \in \mathcal{M}_+(S)$, the support $\text{supp}(\mu)$ is the locus of points $s' \in S$ such that every open neighborhood of s' has a nonzero measure with respect to μ . A pairing $\langle \cdot, \cdot \rangle$ may be defined between $f \in C(S)$ and $\mu \in \mathcal{M}_+(S)$ by $\langle f, \mu \rangle = \int_S f(s) d\mu(s)$. This pairing defines an inner product between $C_+(S)$ and $\mathcal{M}_+(S)$ when the set S is compact. The mass of a measure $\mu \in \mathcal{M}_+(S)$ is $\langle 1, \mu \rangle$, and μ is a probability measure if $\langle 1, \mu \rangle = 1$. The Dirac delta $\delta_{s'}$ is the unique probability supported only at $s' \in S$, with $\forall f \in C(S) : \langle f, \delta_{s'} \rangle = f(s')$. Given a curve $s : [0, T] \times S$, the occupation measure μ_s of $s(t)$ in the times $[0, T]$ is the unique measure satisfying $\forall v \in C([0, T] \times S) : \langle v(t, s), \mu_s \rangle = \int_0^T v(t, s(t)) dt$.

2.3 Sum of Squares

Verifying that a polynomial $p \in \mathbb{R}[x]$ is nonnegative $\forall x \in \mathbb{R}^n$ is generically an NP-hard problem (except for p quadratic, univariate, or bivariate quartic) [22]. A sufficient condition for p to be nonnegative is if there exists N factors $\{p_k \in \mathbb{R}[x]\}_{k=1}^N$ such that $p = \sum_{k=1}^N p_k(x)^2$. Such a p is therefore called an SOS polynomial. The cone of SOS polynomials is $\Sigma[x]$, and the subset of degree $\leq 2d$ SOS polynomials is $\Sigma[x]_d \subset \Sigma[x]$. To each polynomial $p \in \Sigma[x]_d$, there exists an s -dimensional vector of polynomials $v(x)$ (e.g. monomials up to degree d) and a PSD Gram matrix $Q \in \mathbb{S}_+^s$ such that $p(x) = v(x)^T Q v(x)$. When the monomial basis is used, the Gram matrix has dimension $\binom{n+d}{d}$. Verification of $p \in \Sigma[x]_{2d}$ at fixed degree can be performed by solving an SDP. The per-iteration scaling of Interior Point Methods for solving this SDP rises in a jointly polynomial manner with n and d (with $O(n^{6d})$ and $O(d^{4n})$) [23] [24].

A BSA set $\mathbb{K} \in \mathbb{R}^n$ is a set formed by the locus of a finite number of inequality and equality constraints of bounded degree:

$$\mathbb{K} = \{x \mid \forall i = 1..N_g : g_i(x) \geq 0, \forall i = 1..N_h : h_i(x) = 0\}. \quad (2)$$

A sufficient condition for $p \in \mathbb{R}[x]$ to be nonnegative over \mathbb{K} is that there exists multipliers $\sigma_0, \sigma_i, \phi_j$ such that [25]

$$p(x) = \sigma_0(x) + \sum_i \sigma_i(x) g_i(x) + \sum_j \theta_j(x) h_j(x) \quad (3a)$$

$$\exists \sigma_0(x) \in \Sigma[x], \quad \sigma_i(x) \in \Sigma[x], \quad \phi_j \in \mathbb{R}[x]. \quad (3b)$$

The Weighted Sum of Squares (WSOS) cone $\Sigma[\mathbb{K}]$ is the set of polynomials that admit a representation as in (3). The truncated WSOS set $\Sigma[\mathbb{K}]_d$ is the set of polynomials where the certificate in (3) has $\deg \sigma_0 \leq 2d, \forall i : \deg \sigma_i g_i \leq 2d$, and $\forall j : \deg \phi_j h_j \leq 2d$. Verification of $p \in \Sigma[\mathbb{K}]$ could require multipliers that have an exponential degree in n and $\deg p$ [26].

The BSA set \mathbb{K} is *Archimedean* if there exists $R \in [0, \infty)$ such that $R - \|x\|_2^2 \in \Sigma[\mathbb{K}]$. Archimedeaness is a stronger property than compactness [27]. If there exists a known \tilde{R} verifying compactness such that $\mathbb{K} \subseteq \{x \in \mathbb{R}^n \mid \|x\|_2^2 \leq \tilde{R}\}$, then the compact set \mathbb{K} may be rendered Archimedean by adding the redundant ball constraint $\tilde{R} - \|x\|_2^2 \geq 0$ to the list of constraints in (2). When \mathbb{K} is Archimedean, the Putinar Positivstellensatz states that every positive polynomial over \mathbb{K} is a member of $\Sigma[\mathbb{K}]$ [25, Theorem 1.3]. The moment-SOS hierarchy is the process of increasing the degree d in $\Sigma[\mathbb{K}]_d$ to eventually include the set of all positive polynomials.

3 Crash-Safety Program

This section applies peak-minimizing control conversion to the general crash-safety task in (1). The specific crash-safety task used in the data-driven framework will be subsequently considered in Section 4.

3.1 Motivating Example

This subsection provides an example demonstrating how (1) can be used for safety quantification. The Flow dynamics from [8] are

$$\dot{x} = \begin{bmatrix} x_2 \\ -x_1 - x_2 + \frac{1}{3}x_1^3 \end{bmatrix}. \quad (4)$$

This example will be perturbed (4) by an uncertainty process restricted to $\forall t: w(t) \in [-1, 1]$:

$$\dot{x} = \begin{bmatrix} x_2 \\ -x_1 - x_2 + \frac{1}{3}x_1^3 \end{bmatrix} + w \begin{bmatrix} 0 \\ 1 \end{bmatrix}. \quad (5)$$

Trajectories evolve over a time horizon of $T = 5$ in the state set $X = [-0.6, 1.75] \times [-1.5, 1.5]$ with a maximum corruption of $J_{\max} = 2$. System dynamics are illustrated by the blue streamlines in Figure 1. The red half-circle is the unsafe set $X_u = \{x \mid x_2 \leq -0.5, (x_1 - 1)^2 + (x_2 + 0.5)^2 \leq 0.5^2\}$. Two trajectories of this system are highlighted. The green trajectory starts from the top initial point $X_0^1 = [0; 1]$, and the yellow trajectory starts from the bottom initial point $X_0^2 = [1.2966 - 1.5]$. The distance of closest approach to X_u is 0.2498 for both trajectories (matching up to four decimal places). The 0.2498-contour of constant distance is displayed by the red curve surrounding X_u .

The OCP solver CasADi [28] returns approximate bounds for (1) of $Q^* \approx 0.3160$ for X_0^1 (green) and $Q^* \approx 0.6223$ for X_0^2 (yellow). The points (X_0^1, X_0^2) return nearly identical distances of closest approach, but X_0^2 may be judged as safer than X_0^1 under the disturbance model in (4) due to its higher crash-bound value. Degree-4 SOS tightenings of (6) developed in the sequel return lower bounds of 0.3018 and 0.5273 respectively.

3.2 Assumptions

We will require assumptions in order to ensure that the developed infinite-dimensional convex LP will have the same optimal value as (1). These assumptions compactness, convexity, and regularity assumptions arise from the optimal control work in [29].

- A1 The sets $[0, T], [0, J_{\max}], X, W, X_u, X_0$ are all compact.
- A2 The image $f(t, x, W)$ is convex for each fixed (t, x) .
- A3 The dynamics function $f(t, x, w)$ is Lipschitz in the compact domain $[0, T] \times X \times W$.
- A4 If $x(t \mid x_0, w) \in \partial X$ for some $t \in [0, T]$, $x_0 \in X_0$, $w \in W$, then $x(t' \mid x_0) \notin X \forall t' \in (t, T]$.

A1 ensures boundedness and boundary-inclusion of all relevant sets. A2 guarantees that it suffices to analyze trajectories of the differential inclusion $\dot{x} \in \text{conv}(f(t, x, W))$. This paper will generally deal with the case where f is affine in w , so that A2 will therefore be satisfied. A3 ensures Lipschitz regularity (and thus uniqueness) of trajectories given an input $w(\cdot)$. A4 is an assumption of non-return used in [10] that is weaker than ensuring X is an invariant set.

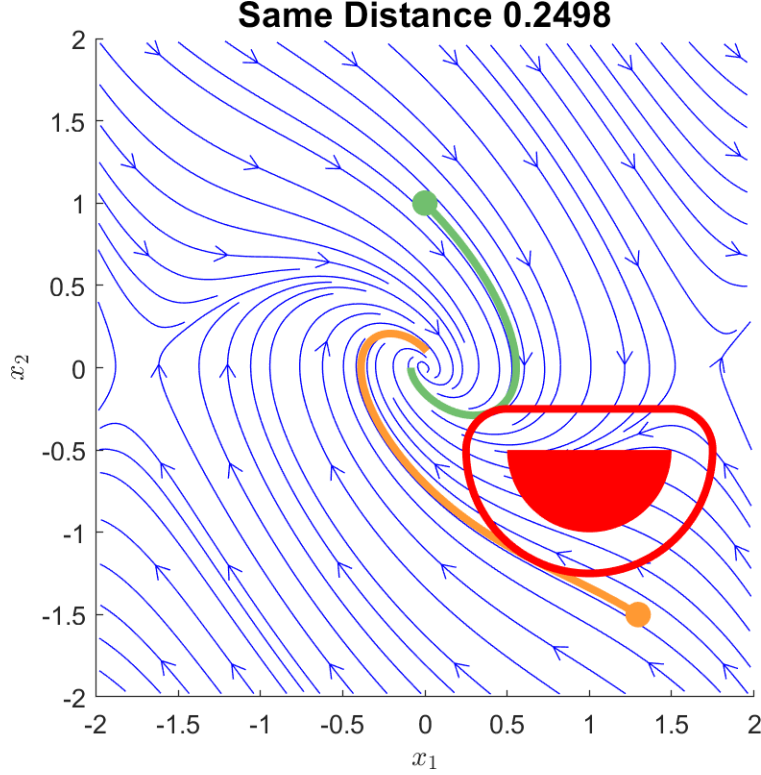


Figure 1: Two trajectories with nearly the same distance but different crash-bounds

3.3 Formulation

We use the peak-minimizing control conversion of [5] on program (1).

Theorem 3.1. *The following program has the same optimal value as (1):*

$$Q_z^* = \inf_{t, x_0, z, w} z \tag{6a}$$

$$\dot{x}(t') = f(t', x(t'), w(t')) \quad \forall t' \in [0, T] \tag{6b}$$

$$\dot{z}(t') = 0 \quad \forall t' \in [0, T] \tag{6c}$$

$$J(w(t')) \leq z \quad \forall t' \in [0, T] \tag{6d}$$

$$x(t \mid x_0, w(\cdot)) \in X_u \tag{6e}$$

$$w(\cdot) \in W, \quad t \in [0, T] \tag{6f}$$

$$x_0 \in X_0, z \in [0, J_{\max}]. \tag{6g}$$

Proof. The parameter z is added as a constant state (6c). This parameter upper-bounds the values of $J(w)$ along trajectories (6d). The objective (6a) therefore infimizes this upper-bound of $J(w)$, forming an equivalence with (1). □

3.4 Crash-Safety Linear Program

This subsection will present infinite-dimensional LP relaxation to (6), and will prove conditions for which the LP relaxations give the same objective value as the original problems in trajectories. First, the following compact support sets involving the input w and peak-bound z must be defined:

$$Z = [0, J_{\max}] \quad \Omega = \{(w, z) \in W \times Z : J(w) \leq z\}. \tag{7}$$

The LP will be posed in terms of an auxiliary function $v(t, x, z) \in C^1$. Consistency of values of v along trajectories of the dynamical system will be enforced through a Lie derivative constraint. This Lie derivative \mathcal{L}_f will be defined as

$$\mathcal{L}_f v(t, x, z, w) = (\partial_t + f(t, x, w) \cdot \nabla_x) v(t, x, z) \quad (8)$$

Our presented LP formulation of the crash-safety OCP in (1):

$$q^* = \sup_{\gamma \in \mathbb{R}, v} \gamma \quad (9a)$$

$$\forall (x, z) \in X_0 \times Z :$$

$$v(0, x, z) \geq \gamma \quad (9b)$$

$$\forall (t, x, z) \in [0, T] \times X_u \times Z$$

$$v(t, x, z) \leq z \quad (9c)$$

$$\forall (t, x, z, w) \in [0, T] \times X \times \Omega$$

$$\mathcal{L}_f v(t, x, z, w) \geq 0 \quad (9d)$$

$$v(t, x, z) \in C^1([0, T] \times X \times Z). \quad (9e)$$

Theorem 3.2. *Under assumptions A1-A4, programs (1) and (9) will have equal objectives $q^* = Q^*$.*

Proof. Program (6) with optimum Q_z^* is a standard-form OCP with free terminal time and zero running cost. Under assumptions A1-A5, Theorem 2.1 of [12] proves that $Q_z^* = q^*$. Section 6.3 of [12] specifically discusses state-dependent controls (e.g. $(w, z) \in \Omega$). Theorem 3.1 provides that $Q^* = Q_z^*$, which together implies that $Q^* = q^*$. \square

The dual LP of (9) may be phrased in terms of an initial measure μ_0 , terminal measure μ_u , and relaxed occupation measure μ :

$$m^* = \inf_{\mu_0, \mu_p, \mu} \langle z, \mu_u \rangle \quad (10a)$$

$$\langle v(t, x, z), \mu_u \rangle = \langle v(0, x, z), \mu_0 \rangle + \langle \mathcal{L}_f v(t, x, z, w), \mu \rangle \quad (10b)$$

$$\langle 1, \mu_0 \rangle = 1 \quad (10c)$$

$$\mu_0 \in \mathcal{M}_+(X \times Z) \quad (10d)$$

$$\mu_u \in \mathcal{M}_+([0, T] \times X_u \times Z) \quad (10e)$$

$$\mu \in \mathcal{M}_+([0, T] \times X \times \Omega). \quad (10f)$$

Constraint (10a) is a Liouville equation involving the Young measure μ [30].

Lemma 3.3. *There exists a feasible solution to (10b)-(10f) under A1-A4.*

Proof. Let $t^* \in [0, T]$ be a stopping time, $x_0 \in X_0$ be an initial condition, and $w(\cdot) \in \mathcal{W}$ be an input such that $x(t^* | x_0, w(\cdot)) \in X_u$. Let z^* be a feasible solution to $\forall t \in [0, t^*] : (z^*, w(t)) \in \Omega$. Then the probability measures can be set to $\mu_0 = \delta_{x=x_0, z=z^*}$ and $\mu_u = \delta_{t=t^*, x=x(t^* | x_0, w(\cdot)), z=z^*}$, and μ can be assigned to the occupation measure of $t \mapsto (t, x(t^* | x_0, w(\cdot)), w(t))$ in the times $[0, t^*]$. \square

Remark 1. *The process of 3.3 to generate a feasible measure solution may be used when only A1 and A4 are active, thus certifying that $m^* \leq Q^*$.*

Theorem 3.4. *Strong duality occurs with $q^* = d^*$ between (10) and (9) under assumptions A1-A4.*

Proof. This holds by standard OCP LP duality arguments from [12, 31, 32], in which feasibility of a measure solution is demonstrated in Lemma 3.3. \square

4 Data-Driven Crash-Safety Analysis

This section motivates crash-safety in the context of data-driven analysis. The cost function J will be interpreted as a measure of alignment with a model class, and the assumption that $J(0) = 0$ will be removed in this section to allow for modeling errors.

4.1 Data-Driven Overview

In this section, we will assume that N_s time-state-derivative data records $\mathcal{D} = \{(t_k, x_k, y_k)\}_{k=1}^{N_s}$ are provided for the true system $\dot{x} = F(t, x)$. The record y_k is a noisy observation of the derivative (value of F) at time t_k and state x_k . The data records in \mathcal{D} are corrupted by L_∞ -bounded uncertainty of intensity ϵ with

$$\forall k = 1..N_s \quad \|y_k - F(t_k, x_k)\|_\infty \leq \epsilon. \quad (11)$$

We are given a dictionary of functions $(f_0, \{f_\ell\}_{\ell=1}^L)$ that are Lipschitz in $[0, T] \times X$ (e.g. monomials). This dictionary of functions will be used to describe the ground-truth (and a-priori unknown) dynamics $F(t, x)$. We are also given the knowledge that there exists at least one ground-truth choice of parameters $w^* \in \mathbb{R}^L$ with

$$F(t, x) = f_0(t, x) + \sum_{\ell=1}^L w_\ell^* f_\ell(t, x). \quad (12)$$

The affine parameters w in the data-driven case will be treated as an uncertainty $w(\cdot)$ from the prior section. Specifically, the data \mathcal{D} will be used to describe a set of parameters w that are consistent with the data up to corruption level z .

In the L_∞ -bounded polytopic framework, the crash-safety problem (6) finds an infimal upper bound on the data corruption needed to crash into the unsafe set:

$$Z^* = \inf_{t, x_0, z, w} z \quad (13a)$$

$$\forall t' \in [0, T] :$$

$$\dot{x}(t') = f_0(t', x) + \sum_{\ell=1}^L w_\ell f_\ell(t', x(t')) \quad (13b)$$

$$\dot{z}(t') = 0 \quad (13c)$$

$$x_0 \in X_0, \quad x(t \mid x_0, w) \in X_u \quad (13d)$$

$$\forall k = 1..N_s : \quad (13e)$$

$$z \geq \|f_0(t_k, x_k) + \sum_{\ell=1}^L w_\ell f_\ell(t_k, x_k) - y_k\|_\infty$$

$$z \in Z, \quad w \in \mathbb{R}^L, \quad t \in [0, T]. \quad (13f)$$

If the returned value of (13) is $Z^* = 0$, then there exists some choice of model parameters w that exactly fit the data \mathcal{D} by (12). Additionally, this choice w renders at least one trajectory $x(\cdot)$ starting from X_0 is unsafe (crashes into X_0). Values of Z^* greater than 0 are a certificate of safety in the model structure. A larger value of Z^* indicates that the data must be increasingly corrupted in order to render any trajectory unsafe. Safety is certified if $Z^* > \epsilon$, though we note that the true value of ϵ may be a-priori unknown.

4.2 Robust Data-Driven Program

We will use the input-affine structure of dynamics and polytopic form of (13f) to form an LP that eliminates the parameter w . This elimination leads to increasingly tractable SOS SDPs. For each $k = 1..N_s$, define the data-record matrices Γ_k , h_k by

$$\Gamma_k = [f_1(t_k, x_k), \dots, f_L(t_k, x_k)] \quad (14a)$$

$$h_k = f_0(t_k, x_k) - y_k. \quad (14b)$$

Letting Γ and h be the vertical concatenations of $\{\Gamma_k\}$ and $\{h_k\}$ respectively, we can define the L_∞ performance function and support set as

$$J(w) = \|\Gamma w - h\|_\infty = \theta(t, x, w), \quad Z = [0, J_{\max}], \quad (15)$$

and the support set for (w, z) from (13f) as

$$\Omega = \left\{ (w, z) \in \mathbb{R}^L \times Z : \begin{array}{l} \Gamma w \leq z \mathbf{1} - h \\ -\Gamma w \leq z \mathbf{1} + h \end{array} \right\}. \quad (16)$$

We will eliminate the w variable from (9d) by introducing new nonnegative multiplier functions $\{\zeta^+, \zeta_j^-\}_{j=1}^{2nT}$. This elimination proceeds using the infinite-dimensional robust counterpart method of [21], which requires that (9d) hold strictly (with a > 0) constraint.

Theorem 4.1. *A strict version of Lie constraint in (9d) may be robustified (will have the same feasibility/infeasibility conditions) into*

$$\forall (t, x, z) \in [0, T] \times X \times Z : \quad \mathcal{L}_{f_0} v - (z\mathbf{1} - h)^T \zeta^+ - (z\mathbf{1} + h)^T \zeta^- > 0 \quad (17a)$$

$$\forall \ell = 1..L : \quad (\Gamma^T)_\ell (\zeta^+ - \zeta^-) + f_\ell \cdot \nabla_x v = 0 \quad (17b)$$

$$\forall j = 1..2nT : \quad \zeta_j^+, \zeta_j^- \in C_+([0, T] \times X \times Z). \quad (17c)$$

Proof. We define the following variables

$$b_0(t, x, z) = \mathcal{L}_{f_0} v(t, x, z) \quad b_\ell(t, x, z) = f_\ell \cdot \nabla_x v(t, x, z) \quad \forall \ell = 1..L \quad (18a)$$

$$A = [-\Gamma; \Gamma] \quad e(z) = [z - h; z + h] \quad (18b)$$

$$K = \prod_{s=1}^{2nT} \mathbb{R}_{\geq 0}. \quad (18c)$$

to express the strict version of (9d) into the form

$$b_0(t, x, z) + \sum_{\ell=1}^L w_\ell b_\ell(t, x, z) > 0 \quad \forall Aw + e(z) \in K. \quad (19)$$

The parameters of (19) are $(t, x, z) \in [0, T] \times X \times Z$. By Theorems 4.2 and 4.3 of [21], sufficient conditions for (17) to equal the strict version of (9d) are that:

R1 K is a convex pointed cone.

R2 $[0, T] \times X \times Z$ is compact.

R3 A is constant in (t, x, z) .

R4 $(e, b_0, \{b_\ell\})$ are continuous in (t, x, z) .

R1 holds because $\mathbb{R}_{\geq 0}^{2nT}$ is a convex and pointed cone. Compactness of $[0, T] \times X$ holds by A1, and compactness of Z holds by A2. R3 is true because Γ is a constant matrix computed from the data in \mathcal{D} from (14a). R4 is satisfied because e is continuous (affine) in z , and $(b_0, \{b_\ell\})$ are continuous given that $v \in C^1$ (9e) and $(f_0, \{f_\ell\})$ are Lipschitz (A3). The theorem is proven because R1-R4 are all fulfilled. \square

Remark 2. *Strictness in (17a) is required to ensure that ζ^\pm may be chosen to be continuous while not adding conservatism. A nonstrict inequality for (17a) may be developed using possibly discontinuous multipliers ζ^\pm .*

Remark 3. *This paper discussed L_∞ -bounded uncertainty, resulting in polytopic decomposition of the Lie constraint by Theorem 4.1. Theorems 4.2 and 4.4 of [21] may be applied when Ω is a more general semidefinite representable set parameterized by z , such as an intersection of ellipsoids for L_2 -bounded uncertainty, or a projection of spectahedra for semidefinite bounded uncertainty.*

5 SOS Programs

This section poses finite-dimensional SOS tightenings to the infinite-dimensional crash-safety programs.

We will require a strengthening of assumptions A1 and A3 in order to use SOS methods for crash-safety:

A5 The sets $(X, X_u, X_0, [0, T], Z, \Omega)$ are all Archimedean BSA sets and the dynamics $f(t, x, w)$ are polynomial.

5.1 Standard Crash-Safety

For a given degree d , define $\tilde{d} = d + \lfloor \deg f/2 \rfloor$ as the dynamics degree of $f(t, x, w)$. The degree- d SOS tightening of program (9) is

$$q_d^* = \max_{\gamma \in \mathbb{R}, v} \gamma \quad (20a)$$

$$v(0, x, z) - \gamma \in \Sigma[X_0 \times Z]_{\leq d} \quad (20b)$$

$$z - v(t, x, z) \in \Sigma[[0, T] \times X_u \times Z]_{\leq d} \quad (20c)$$

$$\mathcal{L}_f v(t, x, z, w) \in \Sigma_{\tilde{d}}[[0, T] \times X \times \Omega] \quad (20d)$$

$$v(t, x, z) \in \mathbb{R}[t, x, z]_{\leq 2d}. \quad (20e)$$

We need to prove boundeness of (10) in order to prove convergence of (20).

Lemma 5.1. *All measures (μ_0, μ_u, μ) in (10) are bounded under A1-A5.*

Proof. We will use the sufficient condition that a measure is bounded if it has finite mass and its support set is compact. All support sets are compact by assumption A1. The measure μ_0 has mass 1 by (10c). Substitution of $v(t, x, z) = 1$ into (10b) results in $\langle 1, \mu_u \rangle = \langle 1, \mu_0 \rangle = 1$, and applying $v(t, x, z) = t$ yields $\langle 1, \mu \rangle = \langle t, \mu_u \rangle \leq T$. \square

Theorem 5.2. *Under assumptions A1-A5, then the sequence of bounds q_d^* will converge as $\lim_{d \rightarrow \infty} q_d^* = Q^*$ to the optimum of (1).*

Proof. This convergence will occur by Corollary 8 of [33], along with convergence in Theorem 3.2, boundeness of measures in 5.1, the infinite-dimensional strong duality Theorem 3.4, and strong duality between their finite-dimensional SDP truncations [14, Arguments from Theorem 4]. \square

5.2 Robust Crash-Safety

We now apply the robust counterpart from (17) to (9) in order to form a SOS program for the L_∞ data-driven scenario. Define $\tilde{d} = d + \max_{\ell \in 0..L} \lfloor \deg f_\ell/2 \rfloor$ as the dynamics degree of (12). The L_∞ -bounded data-driven robust crash-safety SOS tightening at degree d is

$$\tilde{q}_d^* = \max_{\gamma \in \mathbb{R}, v} \gamma \quad (21a)$$

$$v(0, x, z) - \gamma \in \Sigma_d[X_0 \times Z] \quad (21b)$$

$$z - v(t, x, z) \in \Sigma_d[[0, T] \times X_u \times Z] \quad (21c)$$

$$\begin{aligned} \mathcal{L}_{f_0} v - (z\mathbf{1} - h)^T \zeta^+ - (z\mathbf{1} + h)^T \zeta^- \\ \in \Sigma_{\tilde{d}}[[0, T] \times X \times Z] \end{aligned} \quad (21d)$$

$$\forall \ell = 1..L : \quad (21e)$$

$$\text{coeff}_{txz}((\Gamma^+)_\ell(\zeta^+ - \zeta^-) + f_\ell \cdot \nabla_x v) = 0$$

$$v(t, x, z) \in \mathbb{R}[t, x, z]_{\leq 2d}. \quad (21f)$$

$$\forall j = 1..2nT : \quad (21g)$$

$$\zeta_j^+, \zeta_j^- \in \Sigma[[0, T] \times X \times Z]_{\leq \tilde{d}-1}.$$

Theorem 5.3. *Under assumptions A1-A5 and assuming L_∞ uncertainty structure, the sequence of optimal values from (21) will converge as $\lim_{d \rightarrow \infty} \tilde{q}_d^* = Q^*$.*

Proof. The Lie constraint may be robustified by Theorem 4.1. The SOS program in (21) will converge to a strict version of (9) by Theorem 4.4 of [21] under the polynomial v restriction. Strictness is not overly restrictive when performing smooth approximations, as shown in the proof of Proposition 5 in [34]. \square

Remark 4. *The degree of ζ^\pm in (21g) is set to $2(\tilde{d} - 1)$ so as to ensure that $\deg z\mathbf{1}^T \zeta^\pm = 2\tilde{d} - 1 \leq 2\tilde{d}$ in (21d).*

5.3 Computational Complexity

The computational complexity of the SOS Programs (20) and (21) will be compared in terms of the size of their largest PSD Gram matrix. Specifically, an SOS constraint $p(x) \in \Sigma_d[X]$ with $x \in \mathbb{R}^n$ and $\deg p \leq 2d$ has a Gram matrix description of size $\binom{n+d}{d}$, and the per-iteration complexity of interior point methods moment-SOS scales as $O(n^{6d})$ or $O(d^{4n})$ [24].

Program (20) has three WSOS terms, together leading to Gram matrices of maximal size $\binom{n+1+d}{d}$, $\binom{n+2+d}{d}$, and $\binom{n+L+2+\tilde{d}}{d}$ [19, 24]. The performance of SDPs derived from (20) is dominated by the largest size $\binom{n+L+2+\tilde{d}}{d}$ and scales as $(n+L+2)^{6\tilde{d}}$ or $\tilde{d}^{4(n+L+2)}$.

The robustified program in (21) breaks up the Lie constraint's maximal-size Gram matrix dimension $\binom{n+L+2+\tilde{d}}{d}$ into one matrix of size $\binom{n+2+\tilde{d}}{d}$ (21d) and $2nT$ Gram matrices of size $\binom{n+1+\tilde{d}}{d}$ (21g).

Remark 5. *The nonredundant face identification method of [35] requires caution when attempting to reduce complexity of (21). Faces of W that are active at z_1 may no longer be active at $z_2 \geq z_1$ or vice versa [36]. A bound on (21) computed using a subset of faces (constraints) in \mathcal{D} will necessarily be lower than using all faces. This conservatism can be reduced while still eliminating faces by taking the union of active faces of the polytopes in w from $Aw + e \in K$ in (19) at a set of values $z \in (0, J_{\max}]$.*

6 Subvalue Map

Program (9) returns the worst-case crash safety over a set of initial conditions X_0 . We briefly discuss an extension of the crash-safety technique to assessing the safety of arbitrary initial conditions. In the data-driven framework, this could be interpreted as lower-bounding the minimum data corruption needed for a \mathcal{D} -consistent system to crash when starting at any initial point.

6.1 Value Functions

We define the fixed- z value function of (6) (when starting at $X_0 = x'$) as

$$V(x', z) = \begin{cases} z & z \in [0, J_{\max}], \exists t \in [0, T], w(\cdot) \in \mathcal{W} : \\ & x(t \mid x_0, w(\cdot)) \in X_u, J(w(t')) \leq z \forall t' \in [0, t] \\ \infty & \text{otherwise.} \end{cases} \quad (22)$$

The value function $V(x', z)$ is infinite if the control problem of steering a point from x' to X_u is infeasible within the performance budget $J(w) \leq z$. The value function of (6) when restricted to the single initial condition x' is

$$Q(x') = \inf_{z \in [0, J_{\max}]} V(x', z). \quad (23)$$

The value function $Q(x')$ will have an upper bound of J_{\max} if $Q(x')$ is finite, and otherwise will have a value of ∞ . We make no assumptions of continuity or boundedness of $Q(x')$, beyond A1's assurance that J_{\max} is finite.

6.2 Subvalue Approximations

We now use the moment-SOS hierarchy to develop subvalue maps to lower-bound $Q(x')$ from (23).

Proposition 6.1. *Any function $v(t, x, z)$ that satisfies (9c) and (9d) obeys $v(0, x, z) \leq V(x', z)$ from (22) at all $(x, z) \in X \times Z$.*

Proof. Equations (9c) and (9d) are inequality constrained versions of the HJB equality constraints for an optimal value function v^* [11]:

$$v^*(t, x', z) = z \quad \forall (t, x', z) \in [0, T] \times X_u \times Z \quad (24a)$$

$$\min_{w \mid (w, z) \in \Omega} \mathcal{L}_f v^*(t, x', z, w) = 0 \quad \forall (t, x', z) \in [0, T] \times X \times Z. \quad (24b)$$

Refer to the Section 4 of [13] and the proof of Proposition 1 of [34] for the establishment of subvalue relations. \square

Let $\varphi \in \mathcal{M}_+(X)$ be a probability distribution with easily computable moments (e.g., uniform distribution over X when X is a ball or a box), and $Q_{\max} \geq J_{\max}$ be a finite control cap.

Theorem 6.2. *The following program provides a subvalue function $q(x) \leq Q(x)$:*

$$J^* = \sup \int_X q(x) d\varphi(x) \quad (25a)$$

$$q(x) \leq v(0, x, z) \quad \forall (x, z) \in X \times [0, Z_{\max}] \quad (25b)$$

$$q(x) \leq Q_{\max} \quad \forall x \in \text{supp}(\varphi) \quad (25c)$$

$$z \geq v(t, x, z) \quad \forall (t, x, z) \in [0, T] \times X_u \times Z \quad (25d)$$

$$\mathcal{L}_f v(t, x, z, w) \geq 0 \quad \forall (t, x, z, w) \in [0, T] \times X \times \Omega \quad (25e)$$

$$v \in C^1([0, T] \times X \times Z) \quad (25f)$$

$$q \in C(X). \quad (25g)$$

Proof. Proposition 6.1 proves that $v(0, x, z) \leq V(x, z)$ from (22). Constraint (25b) imposes that $q(x) \leq v(0, x, z) \leq V(x, z)$ for all $x \in X$, which implies that $q(x) \leq \inf_z v(0, x, z)$ for all $x \in X$. From the definition of $Q(x')$ in (23) with $Q(x') \leq \inf_z V(x', z)$, it therefore holds that $q(x) \leq Q(x)$ for all $x \in X$. \square

Corollary 1. *The objective J^* from (25) is finite and is bounded above by $J^* \leq Q_{\max}$.*

Proof. Constraint (25c) requires that $q(x)$ is upper-bounded by Q_{\max} . The objective (25a) is therefore upper-bounded by

$$\int_X q(x) d\varphi(x) \leq \int_X Q_{\max} d\varphi(x) \leq Q_{\max} \int_X d\varphi(x) = Q_{\max}, \quad (26)$$

given that φ is a probability distribution. \square

Remark 6. *Let v be a subvalue solution to (25d)-(25f). Any point $x' \in X$ such that $\inf_{z \in Z} v(0, x', z) > J_{\max}$ implies that $Q(x') = \infty$.*

Remark 7. *Without the Q_{\max} cap on the value of q in constraint (25c), the optimal value of (25) could be $J^* = \infty$ if $\exists x' \in X : Q(x') = \infty$.*

Remark 8. *The Lie constraint in (25e) may be robustified through the methods in Section 4 when f is input-affine and W is a semidefinite representable set (e.g., a polytope from the L_∞ data-driven case).*

Define $q_d \in \mathbb{R}[x]_{\leq 2d}, v_d \in \mathbb{R}[t, x, z]_{\leq 2d}$ as the polynomials obtained by solving the degree- d SOS tightening of (25). Let $I_u(x)$ be the indicator function

$$I_u(x) = \begin{cases} 0 & x \in X_u \\ -\infty & x \notin X_u \end{cases}. \quad (27)$$

For a sequence of orders $d' = 1..d$, a parametric function $q_{1:d}$ may be defined as

$$q_{1:d}(x) = \max(I_u(x), \max_{d' \in 1..d} q_{d'}(x)). \quad (28)$$

Definition 6.1 ([37]). *A sequence of continuous functions $\{q_k(x)\}$ converges **almost uniformly** to $Q(x)$ with respect to a measure $\varphi \in \mathcal{M}_+(X)$ if $\epsilon > 0 : \exists A \subseteq X$, such that $q_k \rightarrow Q$ uniformly on $X \setminus A$ and $\varphi(A) < \epsilon$.*

Theorem 6.3. *The function $q_{1:d}(x)$ will converge almost uniformly to $\min(Q_{\max}, Q(x))$ on the state-space $\text{supp}(\varphi) \in X$ as $d \rightarrow \infty$.*

Proof. Let $\tilde{v} \in \mathbb{R}[t, x, z]$ be a polynomial subvalue function that obeys (25d)-(25f). Corollary 2.5 of [37] proves that the parameterized program $q_{1:d}$ will converge φ -almost uniformly to $\min(Q_{\max}, \min_z \tilde{v}(0, x, z))$, resulting in

$$\lim_{k \rightarrow \infty} \int_X |Q(x) - q_k(x)| d\varphi(x) = 0. \quad (29)$$

Increasing the degree of sublevel polynomials \tilde{v} allows for the choice of admissible \tilde{v} such that $\tilde{v}(0, x, z)$ converges in an L^1 -sense to $V(x, z)$ whenever $V(x, z) \leq Q_{\max}$ [34, Propositions 5 and 6], thus proving the theorem. \square

7 Examples

This section demonstrates the utility of the crash-safety framework. Robust decompositions of the Lie constraint are applied in all examples. MATLAB R2021a code to generate examples is available at <https://github.com/Jarmill/crash-safety>. All SDP are generated using YALMIP [38] and solved using Mosek [39]. Finite-degree crash-bounds from (21) are compared against OCP bounds found using the solver CasADi [28].

The examples in 7.1 perform crash safety with respect to applied inputs w when the ground truth system is known. The examples in 7.2 perform data-driven crash-safety analysis.

7.1 Single-Input Subvalue Comparison

This example demonstrates the computation of crash-bounds and the creation of crash-subvalue functionals for system (5) with $J_{\max} = 1$ and $Q_{\max} = 4$. This subvalue is constructed by solving SOS tightenings of (25) in the space $X = [-2, 2]^2$ and in the time horizon $t \in [0, 5]$

7.1.1 Half-Circle

The first part of this example involves the half-circle respect to the unsafe set $X_u = \{x \mid (x_1 + 0.25)^2 + (x_2 + 0.7)^2 \leq 0.5^2, (0.95 + x_1 + x_2)/\sqrt{2} \leq 0\}$. Figure 2 draws the unsafe set X_u in red. The color shading (colorbar) plots $q_{1:5}(x)$ clamped to the range $[0, J_{\max}] = [0, 1]$. The integral objective values of SOS tightening (25) at degrees 1..5 are $J_{1:5}^* = [1.934 \times 10^{-7}, 4.864 \times 10^{-7}, 3.0794, 5.992, 8.260]$.

The black dot in Figure 2 is the specific initial point $X_0 = [1; 0]$. Table 1 lists crash-bounds on (5) starting at X_0 . The subvalue bound (25) is lower than the corresponding degree bounds at the X_0 -specific program (9).

Table 1: Crash-bounds at $X_0 = [1; 0]$ under SOS tightenings

order	1	2	3	4	5
subvalue (25)	1.089×10^{-9}	1.607×10^{-9}	0.1473	0.3392	0.4053
specific (9)	1.117×10^{-7}	0.1843	0.4369	0.5092	0.5118

We now consider worst-case crash-bounds for the half-circle set with respect to the perturbed flow system (5) and the circular initial set $X_0 = \{x \mid 0.4^2 \geq (x_1 - 1)^2 + x_2^2\}$. Crash-bounds as computed by (21) (SOS tightenings to (9)) in degrees 1..5 are $[8.101 \times 10^{-8}, 6.590 \times 10^{-2}, 0.4054, 0.4631, 0.4638]$. The degree-5 lower-bound of 0.4638 should be compared against the numerical bound of 0.4639 produced by CasADi. The numerically solved trajectory (blue curve) is plotted in Figure 3, along with the unsafe set X_u (red half-circle) and the initial set X_0 (black circle). The initial point of the controlled trajectory (blue dot) is $x_0 \approx [1.3424; 0.2069]$.

7.1.2 Moon

The second part of this example has a nonconvex moon-shaped unsafe set

$$X_u = \{x \mid 0.8^2 - (x_1 - 0.4)^2 - (x_2 + 0.4)^2 \geq 0, (x_1 - 0.6596)^2 + (x_2 - 0.3989)^2 - 1.16^2 \geq 0\}. \quad (30)$$

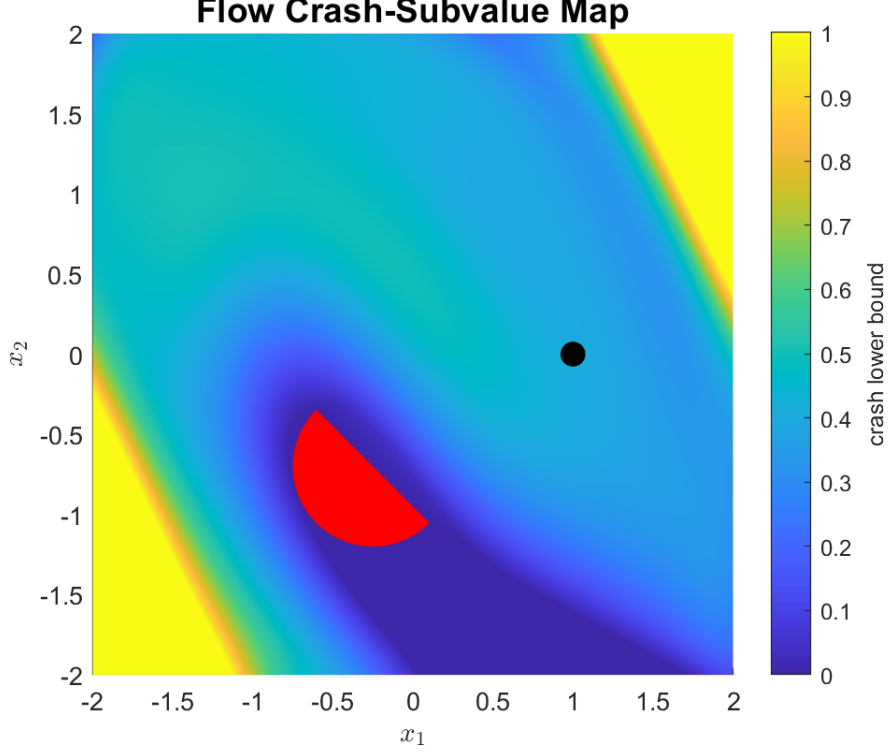


Figure 2: Subvalue function for Flow system (5) between degrees 1..5.

Figure 4 displays a controlled trajectory (blue curve) starting from $X_0 = [0; 0]$ (black circle) and terminating in the X_u (red moon), as computed by CasADi.

Table 2 lists subvalue (25) and specific (9) crash-bounds for $X_0 = [0; 0]$ between degrees 1..5. The objectives of the SOS tightenings to (25) are

$$J_{1..5}^* = [1.973 \times 10^{-7}, 1.323 \times 10^{-7}, 1.027, 3.188, 4.502].$$

Table 2: Crash-bounds at $X_0 = [0; 0]$ for the moon (30) under SOS tightenings

order	2	3	4	5
subvalue (25)	4.652×10^{-10}	-7.861×10^{-2}	-5.692×10^{-3}	7.721×10^{-2}
specific (9)	0.1010	0.2912	0.3216	0.3224

The data from Table 2 at order 1 is subvalue: 8.770×10^{-9} , specific: 2.723×10^{-8} (suppressed for layout/formatting purposes).

Figure 5 plots the subvalue function $q_{1:5}(x)$ from (28) under a cap of $Q_{\max} = 2$ (and $J_{\max} = 1$). All values of $q_{1:5}$ in Figure 5 are clamped to $[0, J_{\max}]$.

7.2 Data-Driven Flow System

Data \mathcal{D} is collected for the Flow system (4) from $N_s = 40$ samples with perfect knowledge in dynamics $\dot{x}_1 = x_2$ and a ground-truth uncertainty bound of $\epsilon = 0.5$ in the coordinate \dot{x}_2 . The noisy derivative data in \mathcal{D} and ground-truth derivatives are drawn in the orange and blue arrows respectively in Figure 6. It is assumed that \dot{x}_2 is described by a cubic polynomial in (x_1, x_2) . The parameterized polytope $\{w \mid Aw \leq b + z\}$ (Ω with fixed z value) has $L = 10$ dimensions and $m = 2nT = 80$. The minimum possible corruption while obeying (12) under the cubic uncertainty model is $\inf_{(w,z) \in \Omega} z = 0.4617$.

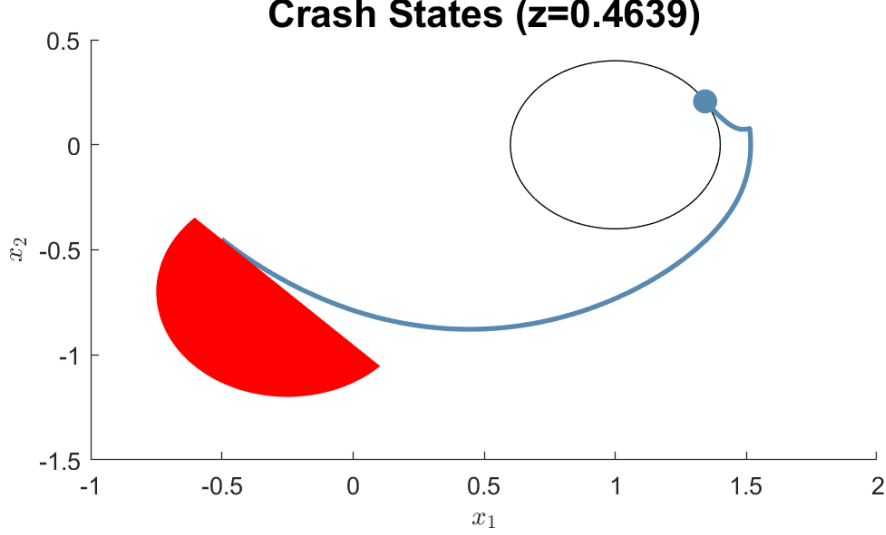


Figure 3: Numerical optimal control yields worst-case $Q^* \approx 0.4639$ for the half-circle X_u

The crash-safety problem (9) and subvalue problem (25) were solved with the unsafe set $X_u = \{x \mid (x_1 + 0.25)^2 + (x_2 + 0.7)^2 \leq 0.5^2, (0.95 + x_1 + x_2)/\sqrt{2} \leq 0\}$ between $t = [0, 5]$ time units in the space $X = \{x \in \mathbb{R}^2 : \|x\|_2^2 \leq 8\}$. The subvalue problem (25) integrates over the uniform measure of the ball X .

Table 3 reports bounds for the crash-corruption $Q(X_0)$ by solving Lie-robustified SOS tightenings of (9) and (25) from degrees 1..4 with $J_{\max} = 1$, $Q_{\max} = 4$. The objective function (integrals of $q(x)$) for the subvalue (25) are $J_{1:4}^* = [0.2193, 3.8185, 7.8326, 18.5945]$. The subvalue-estimated control cost at X_0 between degrees 1..4 is 0.3399 by Equation (28). The subvalue-estimated bound is valid for all $x \in X$, and is therefore lower than the bound $q_4^* = 0.5499$ from (9) that focuses exclusively on the initial point X_0 .

Table 3: Data-Driven Crash-bounds at $X_0 = [1; 0]$ under SOS tightenings

order	1	2	3	4
specific (9)	0.0582	0.4423	0.4864	0.5499
subvalue (25)	6.180×10^{-3}	0.1829	0.3399	0.3399

Figure 7 plots the subvalue function from (28) on the data-driven flow system. Subvalues in the plot are clamped to the range $[0, J_{\max}] = [0, 1]$.

Safety of trajectories starting in X_0 is certified because the crash-bound $\tilde{q}_4^* = 0.5499$ is greater than the ground-truth uncertainty-bound $\epsilon = 0.5$.

The CasADi optimal control suite [28] was used to numerically solve the crash program (1), and the produced trajectory is visualized in Figure 8. The numerical crash-bound of $q^{\text{CasADI}} = 0.5499$ is approximately equal (up to four decimal places) to the crash-bound $q_4^* = 0.5499$.

The left plot of figure 9 shows the applied control of the $L = 10$ inputs. The right plot demonstrates how the polytopic input constraint is obeyed with respect to the crash bound $q^{\text{CasADI}} = 0.5499$ (upper and lower black lines).

These crash-bounds should be compared against the L_2 distance estimates of $c_{1:5}^* = [1.698 \times 10^{-5}, 0.1936, 0.2003, 0.2009, 0.2013]$ from Section 6.3 of [21]. The distance estimates do not indicate that adding an additional budget of 0.0499 constraint violation will cause at least one trajectory to enter the unsafe set.

8 Conclusion

This paper utilized peak minimizing control in order to perform safety analysis. The returned values from SOS programs are lower-bounds on the maximal control effort needed to crash into the unsafe set. Crash-safety adds a new perspective on the safety of trajectories, covering some of the blind spots of distance

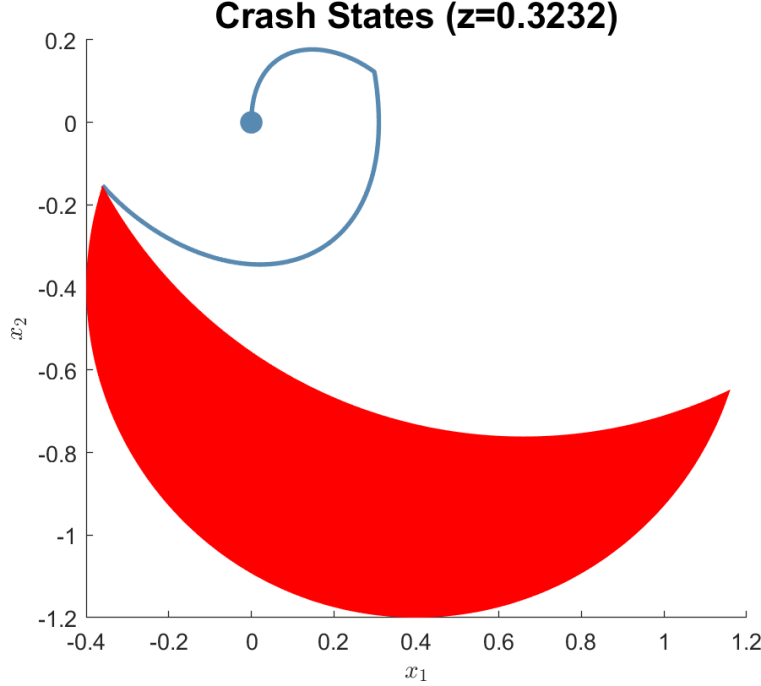


Figure 4: Numerical optimal control yields $Q^* \approx 0.3232$ for the moon X_u

estimation and safety margins. Crash-safety may be applied in the context of data-driven systems analysis, by quantifying the minimum tolerable corruption in an uncertainty model before a trajectory is at risk of being unsafe.

Future work involves attempting to reduce computational burden of the Crash programs (20) by identifying new kinds of structure (in addition to robust decompositions) to hopefully allow for real-time computation. Other extensions could include applying these methods to other classes of systems (e.g., discrete-time, hybrid), and creating a stochastic interpretation of crash-safety.

Acknowledgements

The authors thank Necmiye Ozay and Alain Rapaport for discussions regarding crash-safety and peak-minimizing control.

References

- [1] R. B. Vinter, “Minimax optimal control,” *SIAM journal on control and optimization*, vol. 44, no. 3, pp. 939–968, 2005.
- [2] E. Molina and A. Rapaport, “An optimal feedback control that minimizes the epidemic peak in the SIR model under a budget constraint,” *Automatica*, vol. 146, p. 110596, 2022.
- [3] P. Lu and N. X. Vinh, “Minimax optimal control for atmospheric fly-through trajectories,” *Journal of Optimization Theory and Applications*, vol. 57, no. 1, pp. 41–58, 1988.
- [4] H. Kreim, B. Kugelmann, H. J. Pesch, and M. H. Breitner, “Minimizing the Maximum Heating of a Reentering Space Shuttle: An Optimal Control Problem with Multiple Control Constraints,” *Optimal Control Applications and Methods*, vol. 17, no. 1, pp. 45–69, 1996.

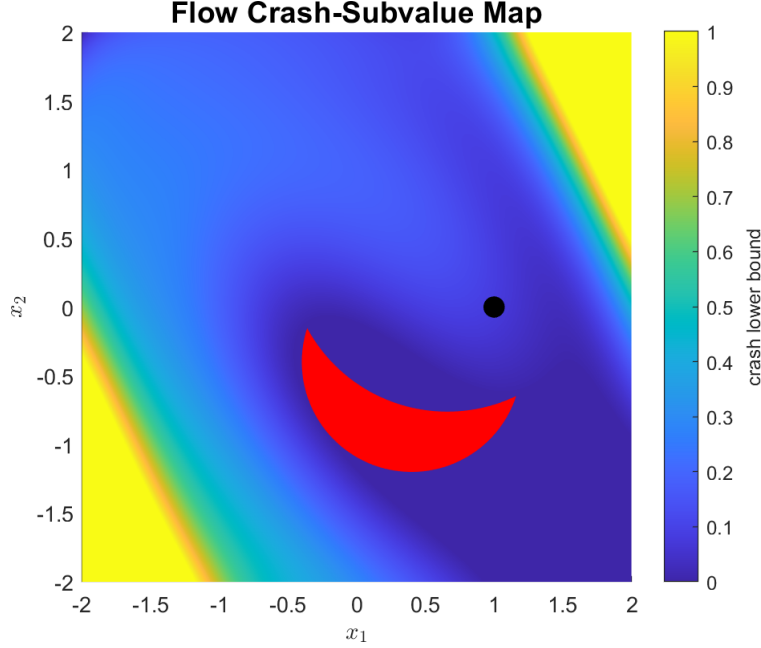


Figure 5: Subvalue map for the moon (30) on the flow system (5)

- [5] E. Molina, A. Rapaport, and H. Ramírez, “Equivalent Formulations of Optimal Control Problems with Maximum Cost and Applications,” *Journal of Optimization Theory and Applications*, vol. 195, no. 3, pp. 953–975, 2022.
- [6] S. Prajna and A. Jadbabaie, “Safety Verification of Hybrid Systems Using Barrier Certificates,” in *International Workshop on Hybrid Systems: Computation and Control*. Springer, 2004, pp. 477–492.
- [7] S. Prajna, “Barrier certificates for nonlinear model validation,” *Automatica*, vol. 42, no. 1, pp. 117–126, 2006.
- [8] A. Rantzer and S. Prajna, “On Analysis and Synthesis of Safe Control Laws,” in *42nd Allerton Conference on Communication, Control, and Computing*. University of Illinois, 2004, pp. 1468–1476.
- [9] J. Miller, D. Henrion, and M. Sznaier, “Peak Estimation Recovery and Safety Analysis,” *IEEE Control Systems Letters*, vol. 5, no. 6, pp. 1982–1987, 2020.
- [10] J. Miller and M. Sznaier, “Bounding the Distance to Unsafe Sets with Convex Optimization,” 2021, arXiv: 2110.14047.
- [11] D. Liberzon, *Calculus of Variations and Optimal Control Theory: A Concise Introduction*. Princeton university press, 2011.
- [12] R. Lewis and R. Vinter, “Relaxation of Optimal Control Problems to Equivalent Convex Programs,” *Journal of Mathematical Analysis and Applications*, vol. 74, no. 2, pp. 475–493, 1980.
- [13] D. Henrion, J. B. Lasserre, and C. Savorgnan, “Nonlinear optimal control synthesis via occupation measures,” in *2008 47th IEEE Conference on Decision and Control*. IEEE, 2008, pp. 4749–4754.
- [14] D. Henrion and M. Korda, “Convex Computation of the Region of Attraction of Polynomial Control Systems,” *IEEE TAC*, vol. 59, no. 2, pp. 297–312, 2013.
- [15] M. Korda, D. Henrion, and C. N. Jones, “Inner approximations of the region of attraction for polynomial dynamical systems,” *IFAC Proceedings Volumes*, vol. 46, no. 23, pp. 534–539, 2013.

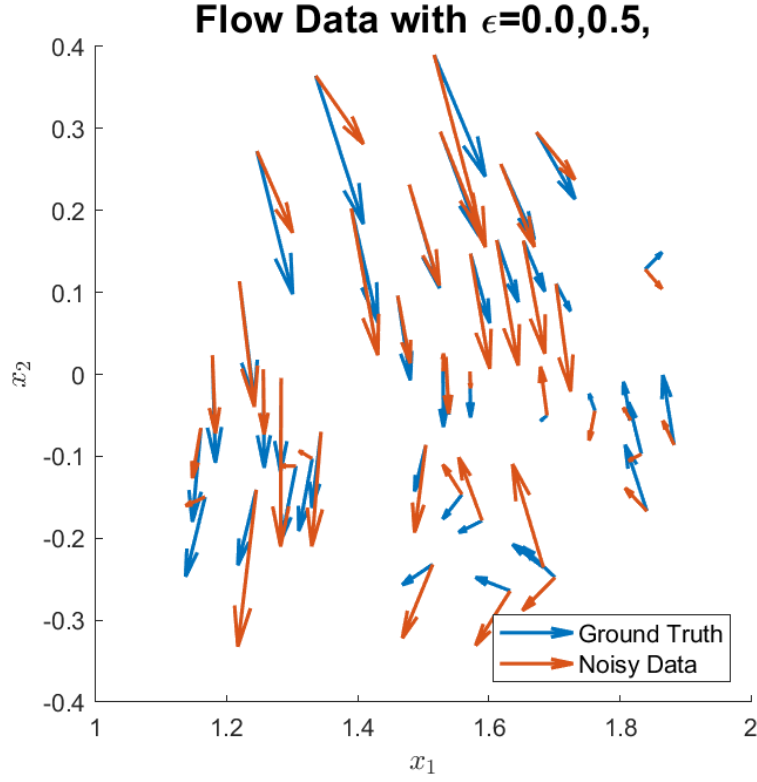


Figure 6: Observed data of the Flow system (4)

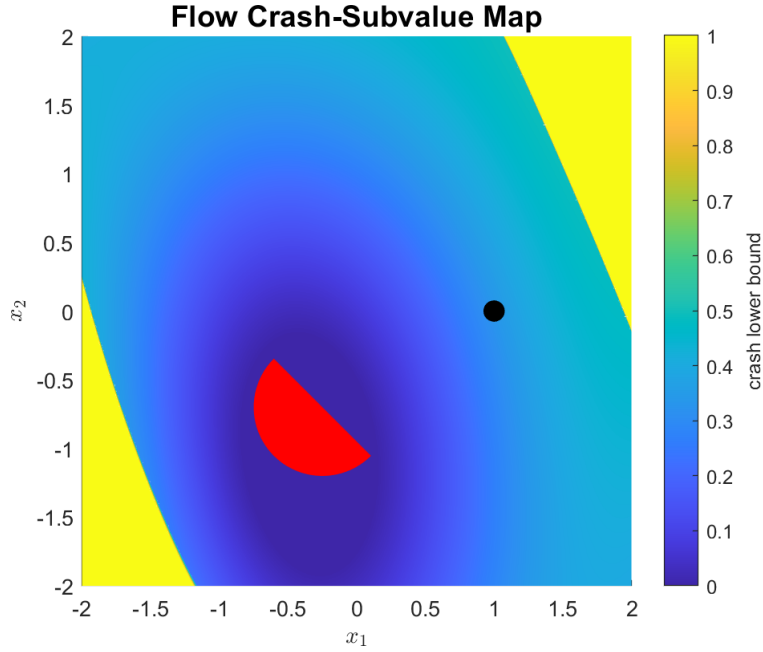


Figure 7: Subvalue for data-driven (4) between degrees 1..4

- [16] G. Fantuzzi and D. Goluskin, “Bounding Extreme Events in Nonlinear Dynamics Using Convex Optimization,” *SIAM Journal on Applied Dynamical Systems*, vol. 19, no. 3, pp. 1823–1864, 2020.
- [17] J. Miller, D. Henrion, M. Sznaier, and M. Korda, “Peak Estimation for Uncertain and Switched Sys-

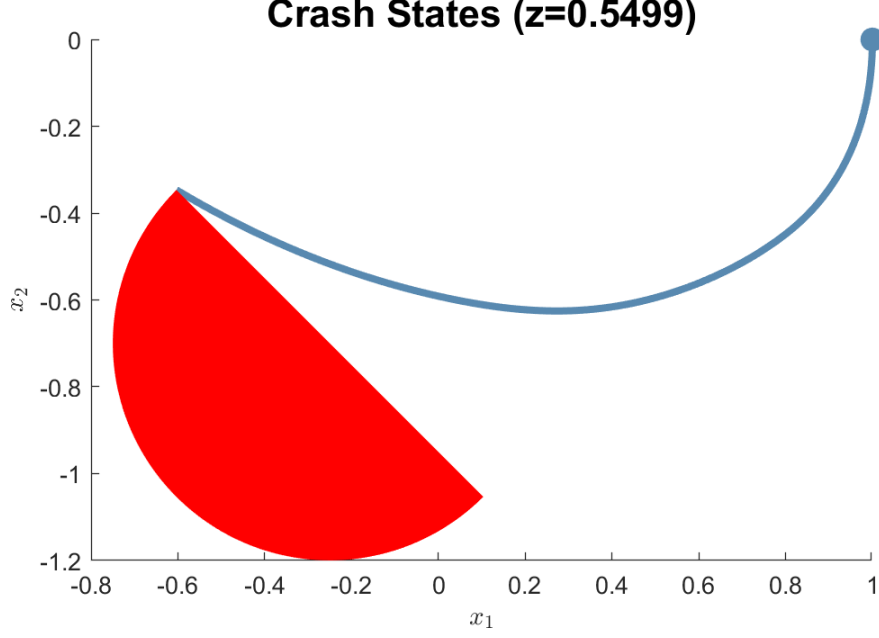


Figure 8: Numerically computed crash-bound for data-driven Flow (4)

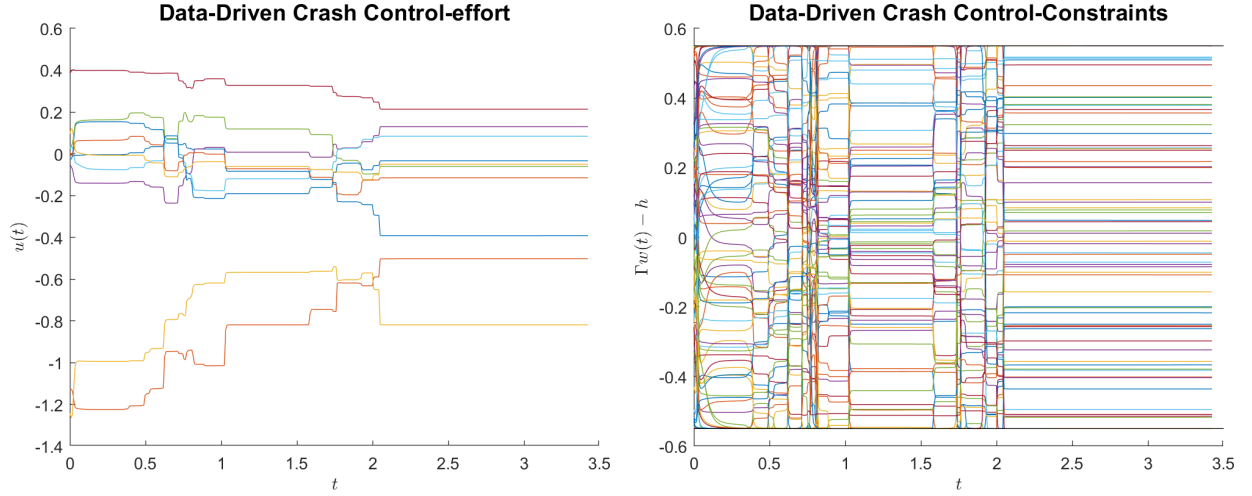


Figure 9: Applied control for the data-driven Flow crash system.

tems,” in *2021 60th IEEE Conference on Decision and Control (CDC)*, 2021, pp. 3222–3228.

- [18] M. Korda, D. Henrion, and C. N. Jones, “Convex computation of the maximum controlled invariant set for polynomial control systems,” *SIAM Journal on Control and Optimization*, vol. 52, no. 5, pp. 2944–2969, 2014.
- [19] J. B. Lasserre, *Moments, Positive Polynomials And Their Applications*, ser. Imperial College Press Optimization Series. World Scientific Publishing Company, 2009.
- [20] A. Ben-Tal, L. El Ghaoui, and A. Nemirovski, *Robust Optimization*. Princeton University Press, 2009, vol. 28.
- [21] J. Miller and M. Sznaier, “Analysis and Control of Input-Affine Dynamical Systems using Infinite-Dimensional Robust Counterparts,” 2023, arxiv:2112.14838.

- [22] D. Hilbert, “Über die darstellung definiter formen als summe von formenquadraten,” *Mathematische Annalen*, vol. 32, no. 3, pp. 342–350, 1888.
- [23] F. Alizadeh, “Interior Point Methods in Semidefinite Programming with Applications to Combinatorial Optimization,” *SIAM J OPTIMIZ*, vol. 5, no. 1, pp. 13–51, 1995.
- [24] J. Miller, T. Dai, and M. Sznaier, “Data-Driven Superstabilizing Control of Error-in-Variables Discrete-Time Linear Systems,” in *2022 61st IEEE Conference on Decision and Control (CDC)*, 2022, pp. 4924–4929.
- [25] M. Putinar, “Positive Polynomials on Compact Semi-algebraic Sets,” *Indiana University Mathematics Journal*, vol. 42, no. 3, pp. 969–984, 1993.
- [26] J. Nie and M. Schweighofer, “On the complexity of Putinar’s Positivstellensatz,” *Journal of Complexity*, vol. 23, no. 1, pp. 135–150, 2007.
- [27] J. Cimprič, M. Marshall, and T. Netzer, “Closures of quadratic modules,” *Israel Journal of Mathematics*, vol. 183, no. 1, pp. 445–474, 2011.
- [28] J. A. Andersson, J. Gillis, G. Horn, J. B. Rawlings, and M. Diehl, “CasADi: a software framework for nonlinear optimization and optimal control,” *Mathematical Programming Computation*, vol. 11, pp. 1–36, 2019.
- [29] R. B. Vinter and R. M. Lewis, “The equivalence of strong and weak formulations for certain problems in optimal control,” *SIAM Journal on Control and Optimization*, vol. 16, no. 4, pp. 546–570, 1978.
- [30] L. C. Young, “Generalized Surfaces in the Calculus of Variations,” *Annals of mathematics*, vol. 43, pp. 84–103, 1942.
- [31] R. Vinter, “Dynamic programming for optimal control problems with terminal constraints,” in *Recent Mathematical Methods in Dynamic Programming: Proceedings of the Conference held in Rome, Italy, March 26–28, 1984*. Springer, 1985, pp. 190–202.
- [32] J. B. Lasserre, D. Henrion, C. Prieur, and E. Trélat, “Nonlinear Optimal Control via Occupation Measures and LMI-Relaxations,” *SIAM Journal on Control and Optimization*, vol. 47, no. 4, pp. 1643–1666, 2008.
- [33] M. Tacchi, “Convergence of Lasserre’s hierarchy: the general case,” *Optimization Letters*, vol. 16, no. 3, pp. 1015–1033, 2022.
- [34] M. Jones and M. M. Peet, “Polynomial Approximation of Value Functions and Nonlinear Controller Design with Performance Bounds,” 2021.
- [35] R. Caron, J. McDonald, and C. Ponc, “A degenerate extreme point strategy for the classification of linear constraints as redundant or necessary,” *Journal of Optimization Theory and Applications*, vol. 62, no. 2, pp. 225–237, 1989.
- [36] V. Loechner and D. K. Wilde, “Parameterized polyhedra and their vertices,” *International Journal of Parallel Programming*, vol. 25, pp. 525–549, 1997.
- [37] J. B. Lasserre, “A “Joint+Marginal” Approach to Parametric Polynomial Optimization,” *SIAM Journal on Optimization*, vol. 20, no. 4, pp. 1995–2022, 2010.
- [38] J. Lofberg, “YALMIP : a toolbox for modeling and optimization in MATLAB,” in *ICRA (IEEE Cat. No.04CH37508)*, 2004, pp. 284–289.
- [39] M. ApS, *The MOSEK optimization toolbox for MATLAB manual. Version 9.2.*, 2020. [Online]. Available: <https://docs.mosek.com/9.2/toolbox/index.html>